

This article was downloaded by:

On: 25 January 2011

Access details: *Access Details: Free Access*

Publisher *Taylor & Francis*

Informa Ltd Registered in England and Wales Registered Number: 1072954 Registered office: Mortimer House, 37-41 Mortimer Street, London W1T 3JH, UK



## Liquid Crystals

Publication details, including instructions for authors and subscription information:

<http://www.informaworld.com/smpp/title~content=t713926090>

### Liquid crystalline properties of dissymmetric molecules IV. The substituent effect on thermal properties of nematic and smectic A phases in three aromatic ring systems with ester linkages

Meili Duan<sup>a</sup>; Takeyasu Tasaka<sup>a</sup>; Hiroaki Okamoto<sup>a</sup>; Vladimir F. Petrov<sup>a</sup>; Shunsuke Takenaka<sup>a</sup>

<sup>a</sup> Department of Advanced Materials Science and Engineering, Faculty of Engineering, Yamaguchi University, Tokiwadai 2557, Ube, Yamaguchi 755-8611, Japan,

Online publication date: 06 August 2010

**To cite this Article** Duan, Meili , Tasaka, Takeyasu , Okamoto, Hiroaki , Petrov, Vladimir F. and Takenaka, Shunsuke(2010) 'Liquid crystalline properties of dissymmetric molecules IV. The substituent effect on thermal properties of nematic and smectic A phases in three aromatic ring systems with ester linkages', *Liquid Crystals*, 27: 9, 1195 – 1205

**To link to this Article:** DOI: 10.1080/02678290050122042

**URL:** <http://dx.doi.org/10.1080/02678290050122042>

## PLEASE SCROLL DOWN FOR ARTICLE

Full terms and conditions of use: <http://www.informaworld.com/terms-and-conditions-of-access.pdf>

This article may be used for research, teaching and private study purposes. Any substantial or systematic reproduction, re-distribution, re-selling, loan or sub-licensing, systematic supply or distribution in any form to anyone is expressly forbidden.

The publisher does not give any warranty express or implied or make any representation that the contents will be complete or accurate or up to date. The accuracy of any instructions, formulae and drug doses should be independently verified with primary sources. The publisher shall not be liable for any loss, actions, claims, proceedings, demand or costs or damages whatsoever or howsoever caused arising directly or indirectly in connection with or arising out of the use of this material.

# Liquid crystalline properties of dissymmetric molecules IV. The substituent effect on thermal properties of nematic and smectic A phases in three aromatic ring systems with ester linkages

MEILI DUAN, TAKEYASU TASAKA, HIROAKI OKAMOTO\*,  
 VLADIMIR F. PETROV and SHUNSUKE TAKENAKA

Department of Advanced Materials Science and Engineering,  
 Faculty of Engineering, Yamaguchi University, Tokiwadai 2557, Ube,  
 Yamaguchi 755-8611, Japan

(Received 14 January 2000; accepted 16 March 2000)

This paper describes the effect of substituent and ester linkage on smectic properties for some derivatives of 4-*R*-phenyl 4-(4-octyloxybenzoyloxy)benzoates (**1**), 4-octyloxyphenyl 4-(4-*R*-benzoyloxy)benzoates (**2**), 4-(4-octyloxybenzoyloxy)phenyl 4-*R*-benzoates (**3**), and 4-*R*-phenyl 4-octyloxyphenyl terephthalates (**4**) where *R* = OCH<sub>3</sub>, CH<sub>3</sub>, OC<sub>8</sub>H<sub>17</sub>, C<sub>8</sub>H<sub>17</sub>, halogens, CF<sub>3</sub>, OCF<sub>3</sub>, CN, NO<sub>2</sub>, etc. The thermal properties are discussed in terms of the electrostatic nature of the substituents and the relative orientation of the ester groups with respect to both terminal substituents. The substituent effect on the layer structure of the smectic A phase is also examined by means of a small angle X-ray analysis.

## 1. Introduction

The current aim of liquid crystal chemistry is to find a quantitative correlation between liquid crystalline properties and physical properties such as the electrostatic and geometrical nature of molecule. In the theoretical treatment of liquid crystals, the molecules are regarded as linear rod-like or lath-shaped, and the symmetry of molecule is an inevitable requisite in order to simplify the theoretical consideration [1]. However, most practical liquid crystals are neither rod-like nor lath-shaped and lack symmetry of molecular shape; the physical properties arising from the dissymmetry are very important in determining the liquid crystalline properties. For example, the liquid crystalline properties for 4-alkoxyphenyl 4-*R*<sub>2</sub>-benzoates, one of the classical classes of liquid crystals, are reported in table 1 [2–9].

From table 1, we see some interesting tendencies in the liquid crystalline properties. Firstly, 4-butoxyphenyl 4-octyloxybenzoate shows the phase sequence smectic C (SmC)-smectic A (SmA)-nematic (N)-isotropic (I), while 4-octyloxyphenyl 4-butoxybenzoate shows an N-I transition. This suggests that the relative orientation of

the ester linkage to both alkoxy groups is very important for the origin of smectic phases. Secondly, the halogen derivatives tend to show the SmA phase in contrast to derivatives having a methyl or a methoxy substituent. Usually, the smectic properties of ester compounds have been interpreted in terms of polar interactions around the core involving the polar ester linkages [10, 11]. However, this mechanism is insufficient to interpret these phenomena in the substituted phenyl benzoate compounds; for example, the effect of the alkyl chain length, an important factor, is not taken into consideration. Thus not only the polar interactions but also a subtle change in molecular shape by the alternating linkage must be taken into consideration. Similar phenomena are observed in other systems such as substituted benzylideneaniline compounds [2, 3]. These phenomena thus appear to be quite common in liquid crystals having a dissymmetric core.

In an earlier paper, we showed that phenyl 4-(4-alkoxybenzoyloxy)benzoates tend to form the SmA phase in the earlier homologues, in contrast to 4-alkoxyphenyl 4-(benzoyloxy)benzoates having the same core [12]. This tendency is similar to that seen in the phenyl benzoate derivatives mentioned above. A similar

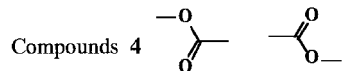
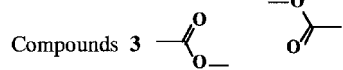
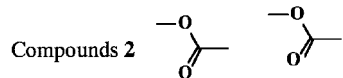
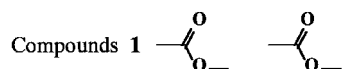
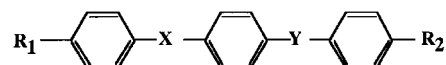
\* Author for correspondence

Table 1. Transition temperatures for substituted phenyl benzoates (°C).

Substituent		X = COO						X = OOC									
R <sub>1</sub>	R <sub>2</sub>	Cr	SmA	N	I	Ref.	Cr	SmA	N	I	Ref.						
C <sub>8</sub> H <sub>17</sub> O <sup>a</sup>	OC <sub>4</sub> H <sub>9</sub>	•	58	•	60	•	89	•	[2]	•	65	—	•	89	•	[2]	
C <sub>10</sub> H <sub>21</sub> O	F	•	42	•	46	•	65	•	[4]	•	79	—	•	83	•	[4]	
C <sub>8</sub> H <sub>17</sub> O	Cl	•	76	•	77	•		•	[5]								
C <sub>8</sub> H <sub>17</sub> O	CN	•	76	—		•	88	•	[6]	•	69	•	87	•	93	•	[7]
C <sub>8</sub> H <sub>17</sub> O	NO <sub>2</sub>	•	50	•	62	•	68	•	[8]	•	67	•	74	•	77	•	[9]

<sup>a</sup> This compound undergoes an SmC–SmA transition at 59°C [2].

phenomenon has been observed in our substituted isomers having two ester linkages, as shown below [13].



R<sub>1</sub> = C<sub>8</sub>H<sub>17</sub>O

R<sub>2</sub> = OC<sub>n</sub>H<sub>2n+1</sub>, C<sub>n</sub>H<sub>2n+1</sub>, halogen, OCF<sub>3</sub>, CF<sub>3</sub>, NO<sub>2</sub>, CN, SCN

The liquid crystalline cores of compounds 1 and 2 are intrinsically dissymmetric, and substitution at both terminal positions will promote the geometrical and electronic dissymmetry. On the other hand, the liquid crystalline cores of 3 and 4 are symmetric, but substitution at both terminal positions will result in the dissymmetry of the entire molecular shape. We have already reported the thermal properties for most of these four compounds [13]. In this paper we describe further thermal and X-ray examination of the liquid crystalline properties of compounds 1–4, and discuss the effect of the substituents and ester linkages on the layer structure of the molecules.

## 2. Experimental

### 2.1. Materials

The homologues of compounds 1–4 were prepared by the conventional method described in our earlier paper [12]; the purity of the products was confirmed by HPLC, <sup>1</sup>H NMR spectroscopy, and DSC using a

‘DSCPURITY’ program (Seiko-denshi Co.). In this work, a purity of more than 99% was achieved.

### 2.2. Characterization

Transition temperatures and latent heats were determined using a Seiko SSC-5200 DSC, with indium (99.9%) as calibration standard (m.p. 156.6°C, 28.4 J g<sup>-1</sup>). The DSC thermogram was operated at a heating or cooling rate of 5°C min<sup>-1</sup>. The mesophases were characterized using a Nikon POH polarizing microscope fitted with a Mettler thermo-control system (FP-900).

X-ray diffraction experiments for the smectic phases were performed using a Rigaku-denki RINT 2200 diffractometer, where CuK<sub>α</sub> (λ = 1.541 Å) was used as an X-ray source. The reflection angle was calibrated by a comparison of both right and left angles. The temperature was controlled using a Rigaku PTC-20A controller. The samples filled in the quartz capillaries (diam. = 1 mm) were oriented by a constant magnetic field (480 G). They were placed along the goniometer axis so that the counter movement in the recording plane allowed scanning of the nematic and smectic reciprocal lattice mode along *q* (*q* = 2*p*/*d* is the reciprocal space vector), i.e. in a direction parallel to the director **n**. The samples were heated to the isotropic temperature, and measurements were carried out during the cooling process.

## 3. Results and discussion

### 3.1. Thermodynamic properties

The SmA phase shows a focal-conic fan and isotropic textures under homogeneous and homeotropic alignments, respectively. The SmC phase for the long alkoxy and alkyl derivatives shows a broken focal-conic fan and schlieren textures under homogeneous and homeotropic alignments, respectively. There was no fundamental difference in the textures through each series of derivatives.

The transition temperatures and entropies for the derivatives of compounds **1–4** are summarized in tables 2–5.

Frequently, parameters such as the nematic–isotropic transition temperature ( $T_{N-I}$ ) and the nematic range ( $T_{N-I} - T_{SmA-N}$ ) have been used as a criterion of liquid crystalline properties. In this paper, we used an  $R$  value defined by McMillan, where  $R$  is the ratio of the SmA–N to N–I transition temperatures, and proposed to be in some way proportional to the smectic interaction strength [21]. Theory predicts that the entropy of the SmA–N transition becomes zero when  $R = 0.88$ , and the transition behaves as a second order type when  $R < 0.88$ . The average effective orders of the cores with the octyloxy group for the clearing point ( $T_{N-I}$  or  $T_{SmA-I}$ ) ( $T_{cl}$ ) and  $R$  are given by:

$$T_{cl}; \mathbf{1} = \mathbf{2} = \mathbf{3} = \mathbf{4}$$

$$R; \mathbf{1} = \mathbf{4} > \mathbf{2} \gg \mathbf{3}$$

$T_{cl}$  is apparently less sensitive to the relative orientation of the ester linkages; in contrast,  $R$  is strongly dependent on their relative orientation. For example, the methoxy derivative of **1** shows mesomorphism of an SmA–N–I type, while the methoxy derivative of **2**

is highly nematogenic, indicating that in the phenyl 4-benzoyloxybenzoate system (the liquid crystal cores of **1** and **2**) the long octyloxy terminal at the 4-benzoyloxy group is indispensable for SmA phase formation, similar to the substituted phenyl benzoate system mentioned above.

The liquid crystalline cores of **3** and **4** are symmetric, so that derivatives with the octyloxy group are assumed to have a similar arrangement in the monolayer SmA phase. Nevertheless, most derivatives of **3** are highly nematogenic in contrast to those of **4**.

From the results for these four isomeric liquid crystal systems, we see that a subtle difference in their molecular structures due to alternation of the two ester groups is important in the formation of the SmA phase [12].

The effective orders for  $T_{cl}$  and  $R$  in relation to substituent are given as follows.

For compounds **1**

$$T_{cl}: \text{CN} > \text{OCH}_3 > \text{NO}_2 > \text{OCF}_3 > \text{Br} > \text{CF}_3 > \text{Cl} \\ > \text{CH}_3 > \text{OC}_8\text{H}_{17} > \text{F} > \text{SCN} > \text{C}_8\text{H}_{17} > \text{H}$$

$$R: \text{OCF}_3, \text{CF}_3 > \text{SCN} > \text{Br} \\ = \text{Cl} = \text{F} > \text{NO}_2 > \text{C}_8\text{H}_{17} > \text{H} > \text{OC}_8\text{H}_{17} > \text{CH}_3 \\ > \text{OCH}_3 > \text{CN}.$$

Table 2. Physicochemical properties of compounds **1**. Cr, SmA, N and I indicate crystal, smectic A, nematic and isotropic phases, respectively.  $\Delta S$  indicates the transition entropy calculated by  $\Delta H/T$ . Layer spacing was measured at  $T_{SmA-N}$  or  $T_{SmA-I} - 10^\circ\text{C}$ .

$R_2$	Transition temperature, $T/^\circ\text{C}$				$\Delta S_{SmA-N}$ or $\Delta S_{SmA-I}$ $\text{J mol}^{-1} \text{K}^{-1}$	$\Delta S_{N-I}$ $\text{J mol}^{-1} \text{K}^{-1}$	$T_{SmA-N}/T_{N-I}$	Layer spacing, $d/\text{\AA}$	Mol. length, $l/\text{\AA}$	$\Delta$ $(d-l)/\text{\AA}$			
	Cr	SmA	N	I									
H	•	118	•	119	•	140	•	4.10	1.71	0.95	28.8	28.5	0.3
OCH <sub>3</sub>	•	107	•	122	•	226	•	0.0	1.21	0.79	30.7	30.6	0.1
OC <sub>8</sub> H <sub>17</sub> <sup>a</sup>	•	84	•	163	•	188	•	2.30	3.89	0.95	38.7	38.8	– 0.1
CH <sub>3</sub>	•	109	•	134	•	195	•	1.00	2.76	0.87		29.3	
C <sub>8</sub> H <sub>17</sub> <sup>b</sup>	•	84	•	160	•	174	•	1.84	3.14	0.97	37.7	37.4	0.3
F	•	120	•	176	•	185	•	4.68	2.17	0.98	28.6	28.8	– 0.2
Cl	•	123	•	200	•	209	•	3.00	1.67	0.98	30.2	29.1	1.1
Br	•	126	•	206	•	214	•	3.68	1.21	0.98	30.7	29.3	1.4
CF <sub>3</sub>	•	126	•	213	—		•	17.3			30.8	29.6	1.2
OCF <sub>3</sub>	•	122	•	216	—		•	13.7			32.1	30.9	1.2
NO <sub>2</sub> <sup>c</sup>	•	114	•	210	•	224	•	0.84	1.42	0.97			
CN <sup>d</sup>	•	116	—		•	229	•					30.0	
SCN <sup>e</sup>	•	110	•	179	•	179	•	8.40		1.0	32.1	30.2	1.9

<sup>a</sup> This compound has a SmC–SmA transition at  $145^\circ\text{C}$  ( $\Delta S = 0.0 \text{ J mol}^{-1} \text{K}^{-1}$ ).

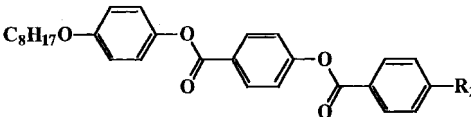
<sup>b</sup> This compound has a SmC–SmA transition at  $88^\circ\text{C}$  ( $\Delta S = 0.0 \text{ J mol}^{-1} \text{K}^{-1}$ ).

<sup>c</sup> See table 6.

<sup>d</sup> Ref. [14].

<sup>e</sup> Ref. [15].

Table 3. Physicochemical properties of compounds 2.



$R_2$	Transition temperature, $T/^\circ\text{C}$				$\Delta S_{\text{SmA-N}}$ or $\Delta S_{\text{SmA-I}}$ $\text{J mol}^{-1} \text{K}^{-1}$	$\Delta S_{\text{N-I}}$ $\text{J mol}^{-1} \text{K}^{-1}$	$T_{\text{SmA-N}}/T_{\text{N-I}}$	Layer spacing, $d/\text{\AA}$	Mol. length $l/\text{\AA}$	$\Delta$ $(d-l)/\text{\AA}$			
	Cr	SmA	N	I									
H	•	118	[• 45]	•	135	•	1.71	0.78					
OCH <sub>3</sub>	•	101	—	•	214	•	1.63		30.1				
OC <sub>8</sub> H <sub>17</sub> <sup>a</sup>	•	84	•	163	•	188	2.30	3.89	0.95	38.2	38.8	− 0.6	
CH <sub>3</sub>	•	112	—	•	189	•	1.50			28.8			
C <sub>8</sub> H <sub>17</sub> <sup>b</sup>	•	93	—	•	175	•	3.51			36.6	37.0	− 0.4	
F	•	114	•	122	•	185	•	0.0	1.76	0.86	30.7	28.2	2.5
Cl	•	119	•	185	•	214	•	0.67	1.42	0.94	31.8	28.4	3.4
Br	•	128	•	192	•	222	•	0.62	1.42	0.94	32.2	28.6	3.6
CF <sub>3</sub>	•	128	•	210	—	•	6.22			31.4	29.8	1.6	
OCF <sub>3</sub>	•	108	•	208	—	•	11.8			31.8	30.2	1.6	
NO <sub>2</sub> <sup>c</sup>	•	101	•	129	•	228	•	0.25	1.38	0.80			
N <sup>d</sup>	•		•	200	•	240	•		0.92		29.2		

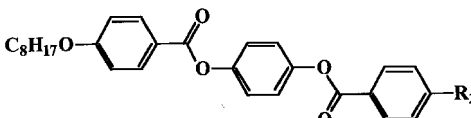
<sup>a</sup> This compound has a SmC–SmA transition at 132°C ( $\Delta S = 0.0 \text{ J mol}^{-1} \text{ K}^{-1}$ ).

<sup>b</sup> This compound has a SmC–SmA transition at 142°C ( $\Delta S = 0.0 \text{ J mol}^{-1} \text{ K}^{-1}$ ).

<sup>c</sup> This compound has a SmA–SmA transition at 109°C ( $\Delta S = 0.0 \text{ J mol}^{-1} \text{ K}^{-1}$ ), see table 6.

<sup>d</sup> Ref. [17].

Table 4. Physicochemical properties of compounds 3.



$R_2$	Transition temperature, $T/^\circ\text{C}$				$\Delta S_{\text{SmA-N}}$ or $\Delta S_{\text{SmA-I}}$ $\text{J mol}^{-1} \text{K}^{-1}$	$\Delta S_{\text{N-I}}$ $\text{J mol}^{-1} \text{K}^{-1}$	$T_{\text{SmA-N}}/T_{\text{N-I}}$	Layer spacing, $d/\text{\AA}$	Mol. length, $l/\text{\AA}$	$\Delta$ $(d-l)/\text{\AA}$			
	Cr	SmA	N	I									
H	•	117	—	•	141	•	2.42						
OCH <sub>3</sub>	•	124	—	•	224	•	2.42			30.7			
OC <sub>8</sub> H <sub>17</sub> <sup>a</sup>	•	122	—	•	194	•	4.51			39.4			
CH <sub>3</sub>	•	102	—	•	199	•	2.34			29.5			
C <sub>8</sub> H <sub>17</sub> <sup>b</sup>	•	101	—	•	176	•	3.80			38.3			
F	•	122	—	•	193	•	2.13			30.2	28.7	1.5	
Cl	•	168	—	•	217	•	1.42			30.8	29.1	1.7	
Br	•	175	—	•	217	•	1.63				29.2		
CF <sub>3</sub>	•	190	•	212	—	•	13.4			31.6	29.6	2.0	
OCF <sub>3</sub>	•	149	•	203	•	209	•	3.01	2.09	0.98	32.2	30.9	1.3
NO <sub>2</sub> <sup>c</sup>	•	165	•	239	•	246	•	1.55	1.76	0.99			
CN <sup>d</sup>	•	140	•	193	•	155	•		0.88		29.9		

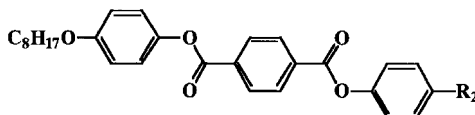
<sup>a</sup> This compound has a SmC–N transition at 126°C ( $\Delta S = 8.03 \text{ J mol}^{-1} \text{ K}^{-1}$ ).

<sup>b</sup> This compound has a SmC–N transition at 118°C ( $\Delta S = 6.40 \text{ J mol}^{-1} \text{ K}^{-1}$ ).

<sup>c</sup> See table 6 ref. [18].

<sup>d</sup> Ref. [19].

Table 5. Physicochemical properties of compounds 4.



$R_2$	Transition temperature, $T/^\circ\text{C}$					$\Delta S_{\text{SmA-N}}$ OR $\Delta S_{\text{SmA-I}}$ $\text{J mol}^{-1} \text{K}^{-1}$	$\Delta S_{\text{N-I}}$ $\text{J mol}^{-1} \text{K}^{-1}$	$T_{\text{SmA-N}}/T_{\text{N-I}}$	Layer spacing, $d/\text{\AA}$	Mol. length, $l/\text{\AA}$	$A$ $(d-l)/\text{\AA}$
	Cr	SmA	N	I							
H <sup>a</sup>	•	154	[• 130]	(• 140)	•			[0.98]			
OCH <sub>3</sub>	•	167	—	• 218	•		1.21			30.4	
OC <sub>8</sub> H <sub>17</sub> <sup>b</sup>	•	144	• 183	• 191	•	1.30	4.39	0.98	36.8	39.0	- 2.2
CH <sub>3</sub>	•	140	—	• 187	•		1.76			29.3	
C <sub>8</sub> H <sub>17</sub> <sup>c</sup>	•	138	• 167	• 175	•	2.47	4.47	0.98	36.2	37.9	- 1.7
F	•	173	• 196	—	•	4.47			30.0	28.5	1.5
Cl	•	195	• 222	—	•	4.85			30.7	28.9	1.8
Br	•	206	• 228	—	•	7.40			31.3	29.0	2.3
OCF <sub>3</sub>	•	193	• 225	—	•	14.4			31.5	30.7	0.8
NO <sub>2</sub> <sup>d</sup>	•	153	• 190	• 220	•	0.25	1.42	0.94			
CN <sup>e</sup>	•	148	• 158	• 233	•			0.85		29.7	
SCN <sup>f</sup>	•	138	• 173	• 178	•	4.60		0.99	32.5	30.4	2.1

<sup>a</sup> The SmA–N transition temperature was extrapolated from the binary phase diagram for the butoxy derivative of **1**.

<sup>b</sup> This compound has a SmC–SmA transition at 180°C ( $\Delta S = 0.88 \text{ J mol}^{-1} \text{ K}^{-1}$ ).

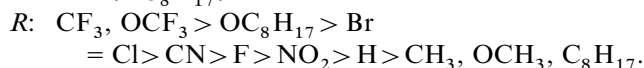
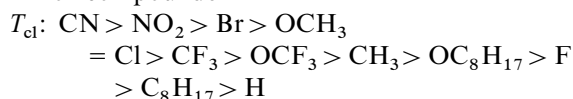
<sup>c</sup> This compound has a SmC–SmA transition at 158°C ( $\Delta S = 0.92 \text{ J mol}^{-1} \text{ K}^{-1}$ ).

<sup>d</sup> See table 6.

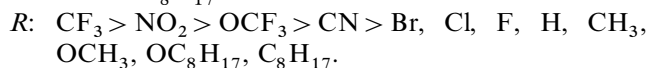
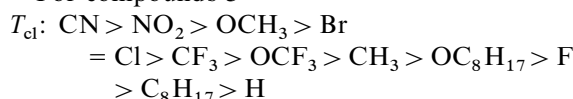
<sup>e</sup> Ref. [19].

<sup>f</sup> This compound has a smectic B–SmA transition at 165°C ( $\Delta S = 62.3 \text{ J mol}^{-1} \text{ K}^{-1}$ ) ref. [20].

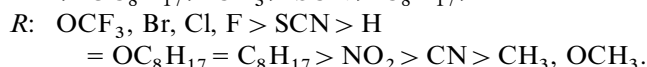
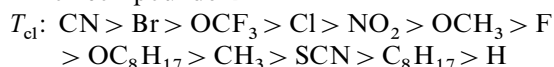
For compounds **2**



For compounds **3**



For compounds **4**



Although the efficiency orders for  $T_{\text{cl}}$  show little difference among the systems, they are essentially consistent with those hitherto reported [22, 23]. The substituent effect on  $R$  is rather different from that on  $T_{\text{cl}}$ , and some apparent trends can be summarized.

Firstly, in series **1** the efficiency for  $R$  reduces in the order  $\text{H} > \text{methyl} > \text{methoxy}$ , while  $\text{methoxy} > \text{methyl} > \text{H}$  for  $T_{\text{cl}}$ . A similar trend is observed in series

**2** and **4**. It is noteworthy that these substituents have an electron-donating nature, enhancing the electron density of the core portion, where the Hammett constant ( $\sigma_{\text{p}}^+$ ) is  $-0.31$  and  $-0.78$  for methyl and methoxy groups, respectively [24]. Secondly, trifluoromethyl and trifluoromethoxy groups notably enhance  $R$ , and induce the SmA phase even in **3**. The characteristic properties of these substituents have been found in the homologues of **2** [25].

Thirdly, the terminal halogens tend to enhance both  $T_{\text{cl}}$  and  $R$ , simultaneously, where the efficiency order is  $\text{Br} > \text{Cl} > \text{F}$ . These substituents have an electron-withdrawing nature, decreasing the electron density of the core moiety, where the Hammett constant ( $\sigma_{\text{p}}^+$ ) is  $-0.07$ ,  $0.11$ , and  $0.15$  for F, Cl, and Br, respectively [24].

Fourth, the effective order of the cyano and nitro groups for  $R$  shows little difference among the systems, indicating that the relative orientation of the ester groups to these substituents also strongly affects the smectic properties. The characteristics of these substituents are that they have simultaneously a strongly electron-withdrawing nature and a large dipole moment ( $-4 \text{ D}$ ).

These results indicate that electron-donating substituents tend to reduce  $R$ , and that electron-withdrawing substituents enhance  $R$ . In the cyano and nitro compounds  $R$  is also affected by the orientation of the ester groups.

### 3.2. X-ray diffraction studies

The X-ray profiles for SmA and SmC phases show a sharp reflection around  $3^\circ$  arising from the  $d_{001}$  direction, and a broad reflection around  $20^\circ$  arising from the  $d_{100}$  direction. In this paper, we study only the thermal behaviour of the  $d_{001}$  peak. The layer spacings converted from the  $d_{001}$  peaks for the octyloxy and octyl derivatives of **1**, **2** and **4** are plotted against temperature in figure 1.

The octyloxy derivative (trace 2) of series **1** has the phase sequence SmC–SmA–N–I, where the SmA phase has a narrow temperature range. The layer spacing decreases as a parabolic curve with decreasing temperature, without showing a plateau region, even in the SmC phase, figure 1(a). This characteristic feature is attributable to the continuous change of the tilt angle of the molecular rotational axis throughout the SmA and SmC phases. The largest layer spacing of 38.2 Å around the SmA–N transition is close to the calculated molecular length, indicating that the SmA phase has a monolayer arrangement.

The octyloxy and octyl derivatives of **4** show similar temperature dependency curves, figure 1(a). Interestingly, however, the maximum layer spacings in the SmA phase are far shorter than the calculated molecular lengths, as shown in table 5. This interesting tendency is observed in the homologous members and is explicable in terms of the specific molecular packing within the smectic layer: details will be presented elsewhere [26].

The octyl derivative of **1** exhibits a wide range SmA phase; the layer spacing in the SmA phase is almost independent of temperature ( $0.3 \text{ \AA}/50^\circ\text{C}$ ), where the layer spacing of 37.7 Å agrees with the calculated molecular length. The octyl derivative of **2** has the phase sequence SmC–N. However, a broad peak arising from the layer structure is observed even in the N phase, where the peak maximum of 36.9 Å agrees with the calculated molecular length. These results indicate that cybotactic

domains having the SmA arrangement are present even in the N phase, while the SmA phase was not observed in either microscopic or DSC measurements.

The temperature dependency of the layer spacings for the trifluoromethyl and trifluoromethoxy derivatives of **2** are shown in figure 1(b). These derivatives preferentially exhibit the SmA phase as shown in table 3, so that their layer spacings are completely independent of temperature, and are longer by 1.6 Å than the calculated molecular lengths. This indicates that these derivatives form a stable smectic layer; any shrinkage of the layer spacing due to thermal fluctuation around the long octyloxy group is negligible in the temperature range 100–200°C.

Figure 2 shows the temperature dependency of the layer spacings for the halogen derivatives of **1–4**. The layer spacings for the Cl derivative of **1** and the F derivative of **4** are almost independent of temperature ( $0.3 \text{ \AA}/70^\circ\text{C}$  and  $0.2 \text{ \AA}/20^\circ\text{C}$ , respectively), and the layer spacings are longer than the calculated molecular lengths. In contrast, the layer spacing for the Br derivative of **2** is longer by 3.6 Å than the calculated molecular length, and shows a notable temperature dependency ( $1.2 \text{ \AA}/50^\circ\text{C}$ ). The F and Cl derivatives of **2** show a similar temperature dependency. These results indicate that the significant temperature dependency arises from the molecular characteristics of **2**, and that a molecular rearrangement occurs in the SmA phase which decreases the layer spacing.

The halogen derivatives of **3** show no smectic phase under microscopic and DSC observation. However, the X-ray profiles of the F and Cl derivatives show a weak and broad reflection at the low temperature region of the N phase, where the peak maxima are longer by 1.5 Å than the calculated molecular lengths. The cybotactic domains accompanying the smectic layer might be present in the low temperature region of the N phase.

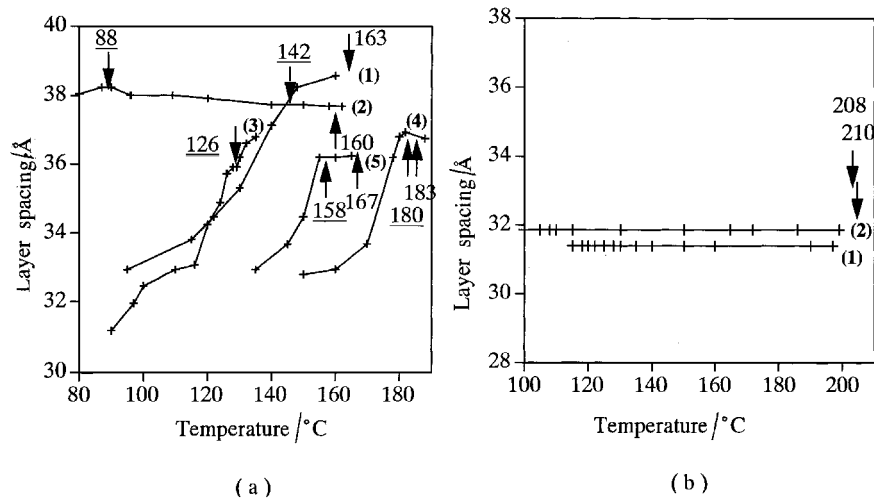


Figure 1. Plots of layer spacing against temperature for: (a) octyloxy (1) and octyl (2) derivatives of **1**, octyl (3) derivative of **2**, octyloxy (4) and octyl (5) derivatives of **4**; (b) trifluoromethyl (1) and trifluoromethoxy (2) derivatives of **2**. Numbers with double underline and underline indicate SmC–N and SmC–SmA transition temperatures, respectively.

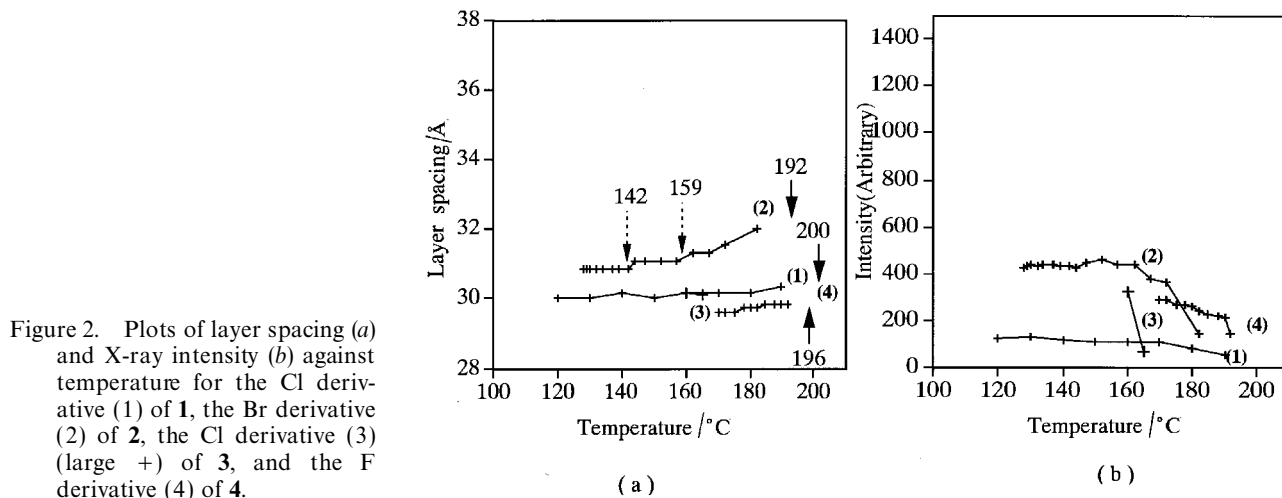


Figure 2(b) shows the temperature dependency of the reflection intensity. The reflection intensity for these derivatives is fairly low, reaching a maximum with decreasing temperature. It is noteworthy that for the Br derivative of **2**, the slight change in layer spacing and the broad increase of reflection intensity occur at the same temperature.

Layer spacings for the thiocyanato derivatives of **1** and **4** are almost independent of temperature, similar to those for the halogen derivatives, and are longer by *c.* 2 Å than the calculated molecular lengths.

The temperature dependencies of the layer spacing and peak intensity for the nitro derivatives show characteristic tendencies, as shown in figure 3. The layer spacing of the SmA phase for the nitro derivative of **1** decreases slowly with decreasing temperature (1.3 Å/100°C), the ratio of the layer spacing to the calculated molecular length varying from 1.22 to 1.18; meanwhile, the intensity of the reflection maxima shows a complex feature with minima at *c.* 159 and 120°C, as shown in figure 3(b).

There is no doubt that certain molecular rearrangements occur around these temperatures, though it was difficult to detect these by either DSC or microscopic measurements. Ratna *et al.* reported that the hexyloxy homologue of **1** shows a similar temperature dependency [14].

Interestingly, the layer spacing for the nitro derivatives of **2** becomes markedly longer with decreasing temperature, where the change is 8.1 Å/60°C, and the ratio of the layer spacing to the calculated molecular length varies from 1.37 to 1.64. A remarkable change of the intensity observed at 110°C in figure 3(b) corresponds to an SmA–SmA transition [13]. The plot shown in figure 3(a), however, did not show a discontinuity around this temperature.

The layer spacings for the nitro derivatives of **3** and **4** also decrease with decreasing temperature; the reductions are 2.0 Å/50°C and 1.5 Å/50°C, respectively. The peak intensity for the nitro derivative of **3** becomes very low at 200°C and shows a complex feature with a minimum at *c.* 170°C. A similar trend was observed in the nitro

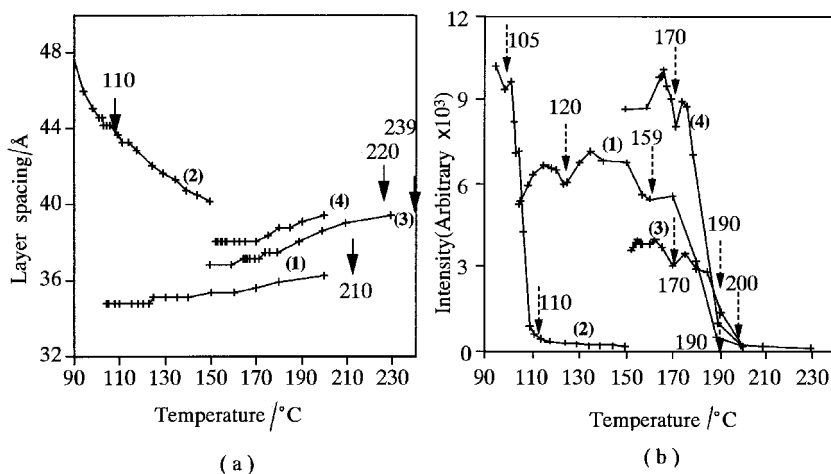


Figure 3. Plots of layer spacing (a) and X-ray intensity (b) against temperature for the nitro derivatives of **1**, **2**, **3** and **4** (correspondingly numbered).



derivative of **4**, where the minimum feature occurred at 170°C. It is assumed that for the nitro derivatives, a complex and continuous change of molecular arrangement occurs in the SmA phase.

The X-ray results are summarized in tables 2–5, where the layer spacings were taken from the maximum values around  $T_{\text{SmA-N}}$ . The X-ray and molecular orbital results for the nitro derivatives are separately summarized in table 6. In the tables, the molecular lengths were estimated by the semi-empirical molecular orbital method (AM1 method in MOPAC ver. 6.0). The calculated molecular lengths in this paper correspond to the longitudinal lengths for the most stable conformation estimated from the AM1 method.

### 3.3. The layer structure of the SmA phase

The SmA phase has been roughly classified into four kinds according to the characteristics of the layer structure: monolayer ( $\text{SmA}_1$ ), bilayer ( $\text{SmA}_2$ ), partially bilayer ( $\text{SmA}_d$ ), and anti-phase ( $\text{Sm}\tilde{\text{A}}$ ) arrangements, where the layer spacings ( $d$ ) of these SmA phases are correlated with the molecular length ( $l$ ) as follows,

$$\text{SmA}_1 \text{ phase } d = l$$

$$\text{SmA}_2 \text{ phase } d = 2l$$

$$\text{SmA}_d \text{ phase } l < d < 2l.$$

The molecular arrangements for dissymmetric molecules are illustrated diagrammatically in figure 4.

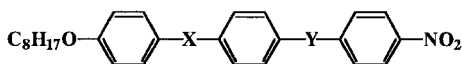
The layer spacings for the octyloxy and octyl derivatives of **1** and **2** are in good agreement with the calculated molecular lengths, so that the molecules in the SmA phase have a monolayer arrangement as shown in figure 4, model (a). Within the smectic layer, the molecules would arrange parallel or anti-parallel side by side, due to the dissymmetric ester groups. In such conditions, intermolecular polar interactions around the carboxyl groups would be attractive in the antiparallel arrangement, and

repulsive in the parallel arrangement. Therefore, the polar interaction model in the antiparallel arrangement would conveniently explain the formation of the SmA phase for the octyloxy and octyl derivatives of **1** and **2**.

On the other hand, the octyloxy derivatives of **3** and **4** are intrinsically symmetric, so that the molecules always arrange parallel side by side and two ester groups are inevitably in a parallel arrangement. According to the general concept, in such conditions the polar interactions around the carboxyl groups are always repulsive. As is evident from comparison of tables 4 and 5, in practice the octyloxy derivative of **4** is superior in smectic properties, and the homologues exhibit SmA and SmC phases from the earlier members. In contrast, the octyloxy homologue of **3** exhibits only the SmC phase with low thermal stability. Thus, the simple model involving polar interactions around the ester groups is insufficient to interpret the smectic properties of all the isomeric ester compounds. It would be reasonable to assume that the alternation of two ester groups would result in a change in the local and entire molecular polarity, affecting the lateral polar interactions within the smectic layer and leading to a change in the entire molecular shape. According to molecular orbital calculations using AM1 method, for example, the diphenyl terephthalate core of **4** is rigid and planar due to a high rotational barrier of  $11.2 \text{ kJ mol}^{-1}$  around the phenyl–COO bond. On the other hand, the 1,4-dibenzoyloxybenzene core of **3** is flexible and non-planar due to the low rotational barrier of  $1.9 \text{ kJ mol}^{-1}$  around the phenyl–OOC bond. The difference in these geometrical factors should be reflected in their mesomorphic properties.

The layer spacings of the trifluoromethyl and trifluoromethoxy derivatives are longer by 0.8–2.0 Å than the calculated molecular lengths, and are independent of temperature. Two kinds of molecular arrangements are possible for these derivatives, as shown in models (b)

Table 6. Molecular lengths and layer spacings for nitro derivatives.  $l$  indicates the calculated molecular length for the most stable conformation of single molecule.  $d$  indicates the observed layer spacing.



- 1** X=COO, Y=COO  
**2** X=OOC, Y=OOC  
**3** X=COO, Y=OOC  
**4** X=OOC, Y=COO

Compound	$l/\text{\AA}$	$d(\text{temp.})/\text{\AA}(\text{^\circ C})$	$d-l/\text{\AA}$	$d/l$	$d(\text{temp.})/\text{\AA}(\text{^\circ C})$	$d-l/\text{\AA}$	$d/l$
<b>1</b>	29.5	34.8(104)	5.3	1.18	36.2(200)	6.7	1.23
<b>2</b>	29.3	48.0(89)	18.7	1.64	40.1(149)	10.8	1.37
<b>3</b>	30.0	36.8(149)	6.8	1.23	39.0(200)	9.0	1.30
<b>4</b>	29.4	38.0(152)	8.6	1.29	39.4(200)	10.0	1.34

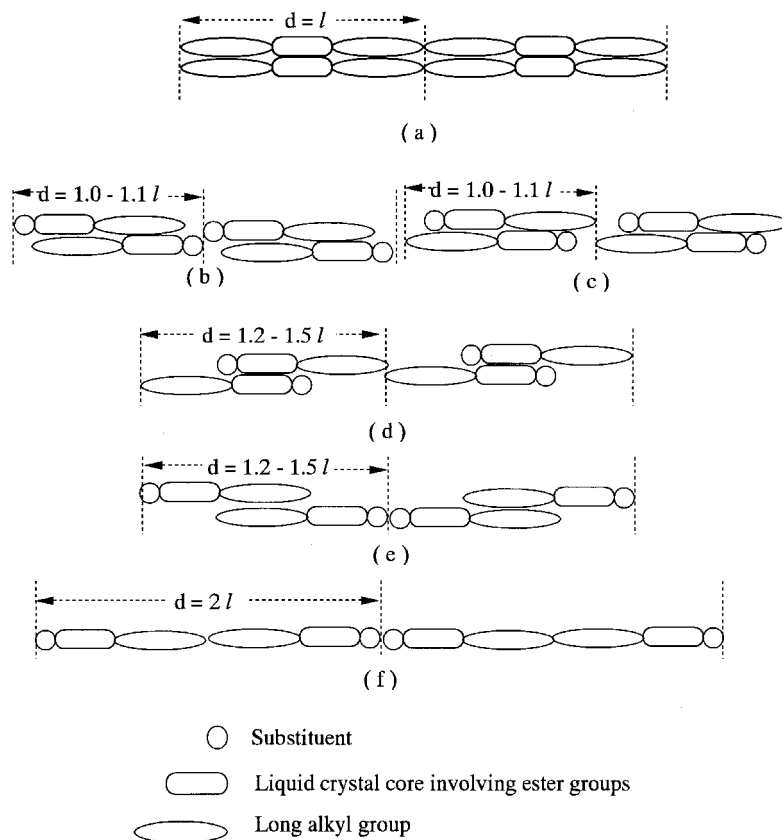


Figure 4. Molecular arrangement models for the SmA phase of dissymmetric molecules.

and (c) in figure 4. It would be reasonable to assume that in dissymmetric liquid crystals the molecules tend to arrange antiparallel on average to take account of dipole correlation and minimization of molecular volume. In model (b), the trifluoromethyl groups are placed outside the smectic layer, and crowd around the boundary of the smectic layer, developing a specific electrostatic sphere, where the alkoxy chains are surrounded by aromatic moieties or *vice versa*. The inter-layer fluorophilic interaction around the layer boundary would facilitate the formation of the layer structure. In model (c) on the other hand, the trifluoromethyl groups are placed inside the smectic layer, and are surrounded by the long hydrocarbon chains. In such circumstances the repulsive interaction between trifluoromethyl and hydrocarbon moieties might be unfavourable for maintaining the layer structure. Therefore model (b) seems to be more suitable for the molecular arrangement of the SmA phase, where the fluorophilic interaction around the layer boundary would stabilize the layer structure. As shown in table 4, these substituents are effective in inducing the SmA phase even in the intrinsically nematogenic **3**.

The layer spacings of the halogen derivatives are also longer by 0–1.4, 2.5–3.6 and 1.5–2.3 Å, respectively, than the calculated molecular lengths for **1**, **2**, and **4**;

in addition, differences are larger in the order of  $\text{Br} > \text{Cl} > \text{F}$ . This order is correlated with the average phenyl–X bond lengths of 1.354, 1.698 and 1.873 Å for F, Cl, and Br, respectively, calculated by the AM1 method. We assume that these molecules arrange antiparallel like model (b) in figure 4, where the terminal halogens are placed around the layer boundary due to specific interactions between the substituents. Such interactions might be weaker than those of trifluoromethyl and trifluoromethoxy groups, so that these groups cannot induce the SmA phase for **3**. Considering that the layer spacings become shorter at lower temperature, the interdigitated molecular arrangement with the long layer spacing is preferentially present in the high temperature region. As mentioned in §1, in 4-*R*-phenyl 4-alkoxybenzoate systems the halogen derivatives show notable smectic properties compared with short chain alkoxy and alkyl derivatives [2, 3]. The characteristic properties of the halogen derivatives should also be attributable to the specific interactions around the terminal halogens.

The thiocyanato derivatives of **1** and **4** exhibit the SmA phase with a layer spacing of *c.* 1.1 that of the molecular length; their physical properties are different from those of the terminal cyano and nitro compounds,

resembling rather the halogen derivatives; polar interactions arising from the thiocyanato group, of course, must play a certain role in stabilization of the layer structure.

There are many papers discussing the thermal properties and layer structures for polar liquid crystals having a terminal cyano or a nitro group [27]. To summarize these, some 4-alkoxy- and 4-alkyl-4'-cyanobiphenyls form antiparallel dimers illustrated in model (*d*) of figure 4, exhibiting a smectic  $A_d$  phase, where electrostatic interactions favour aromatic moieties forming overlapped pairs. Application of this model to the present compounds gives a layer spacing of *c.* 40 Å and a *d/l* ratio of *c.* 1.38. As shown in table 6, the layer spacing is strongly dependent on both orientation of the ester linkages and temperature. For the nitro derivative of **1**, the layer spacing is far shorter than the layer spacing calculated from model (*d*). For the nitro derivatives of **2–4**, on the other hand, the layer spacings in the high temperature region are in good agreement with those (*c.* 40 Å) calculated from model (*d*). A defect of this model is that in the dimers the dipole–dipole interaction between the terminal nitro groups would be very weak, since two nitro groups in the dimer should be further apart than *c.* 15 Å.

The layer spacings for **3** and **4** in the low temperature region are rather shorter than 40 Å, and interestingly that for **2** is far larger. The polar interactions around the ester groups may be responsible for the scattering of the layer spacings.

In connection with model (*b*) (figure 4) for trifluoromethyl and halogen derivatives, the antiparallel dimers model (*e*) is also attractive, and may be close to the  $SmA_d$  model for cyanobiphenyl compounds proposed by Lydon and Coakley [28]. In this model the terminal polar groups closely crowd each other around the layer boundary, and the dipole–dipole interaction between nitro groups will strongly assist the formation of associated dimers, facilitating the formation of the smectic layer, since the terminal nitro groups closely crowd near the layer boundary. In addition, model (*e*) is attractive as an intermediate structure for the process of moving from model (*b*) to (*f*) for the  $SmA_2$  phase sometimes formed in polar liquid crystals. The molecular arrangement corresponding to model (*d*) is found in the layer structure of cyanobiphenyl compounds on  $MoS_2$  or graphite surfaces [29, 30], where the cyanobiphenyl moieties closely crowd each other, probably due to strong dipole–dipole interaction. We have reported that 4- and 3-(2-perfluoroalkylethoxy)nitrobenzenes form antiparallel dimers, assisted by strong dipole–dipole interaction between nitrobenzene moieties, and form a layer structure similar to model (*e*) [31].

The nitro derivative of **2**, having a nonyloxy group instead of octyloxy, has been reported to show the complex phase transition behaviour  $SmC_2-SmA_2-SmC-SmA_1-N_{re}-SmA_d-N_{re}-SmA_d-N-I$ , where the layer spacing shows a remarkable temperature dependency [32–34]. Madhusudana *et al.* reported that 4-alkoxyphenyl 4-(4-cyano-benzoyloxy)benzoates show a similar marked temperature dependency of the layer spacing [35]. Interestingly, the halogen derivatives of **2** show a marked temperature dependency compared with the other derivatives, as shown in figure 2, while their layer spacings become shorter on lowering the temperature, inversely to the nitro derivative. These results indicate that the marked temperature dependency of the layer spacing is an intrinsic nature of 4-alkoxyphenyl 4-(4-*R*-benzoyloxy)benzoates, the liquid crystalline core of **2**. We previously discussed the molecular structures of **1** and **2**, leading to the conclusion that 4-octyloxyphenyl 4-(4-*R*-benzoyloxy)benzoates (the core of **2**) keep the linearity of the entire molecular shape, while 4-*R*-phenyl 4-(4-octyloxybenzoyloxy)benzoates (the core of **1**) are intrinsically bent due to the terminal octyloxy group [12]. Thus the linear shape of **2** might be related to the markable temperature dependency of the layer spacing. In contrast, the intrinsic bent shape of the core of **1** is responsible for the marked smectic properties.

#### 4. Conclusion

The smectic properties of compounds **1–4** are affected by both the electrostatic and structural natures of the core involving two ester linkages; the terminal substituents affect both the thermal stability of  $SmA$  and  $SmC$  phases and the molecular arrangement within the smectic layers. When both terminal substituents are the long alkoxy and alkyl groups, the layer surface is covered with terminal hydrocarbon chains, and molecules tend to form a monolayer arrangement within the layer. When trifluoromethyl and trifluoromethoxy groups, or halogens are substituted at the terminal position, these substituents tend to crowd and form a specific electrostatic sphere around the layer boundary, and electrostatic interactions between substituents stabilize the layer structure, the layer spacing being larger than the fully extended molecular length. For nitro and cyano compounds, the polar interactions form antiparallel dimers around the layer boundary, and stabilize the smectic layer spacing at 1.1–1.4 times the molecular length.

Finally, in the formation of the smectic A phase, we wish to emphasize the importance of both a subtle change in the entire molecular shape due to alternation of the ester groups, and electrostatic interactions between the terminal substituents around the layer boundary.

## References

- [1] CHANDRASEKHAR, S., 1992, *Liquid Crystals* (Cambridge: Cambridge University Press), p. 17.
- [2] DEMUS, D., DEMUS, H., and ZASCHKE, H., 1976, *Flüssige Kristalle in Tabellen* (Leipzig: VEB Deutscher für Grundstoff Industrie).
- [3] DEMUS, D., and ZASCHKE, H., 1984, *Flüssige Kristalle in Tabellen II* (Leipzig: VEB Deutscher Verlag für Grundstoff Industrie).
- [4] NEUBERT, M. E., LEUNG, K., and SAUPE, W. A., 1986, *Mol. Cryst. liq. Cryst.*, **135**, 383; NEUBERT, M. E., LEUNG, K., and SAUPE, W. A., 1993, *Mol. Cryst. liq. Cryst.*, **237**, 47.
- [5] MALTHETE, J. J., BILLARD, J., CANCELL, J. G., and JACQUES, J., 1976, *J. Phys.*, **C3**, **37**, C3-1.
- [6] SCHUBERT, H., SCHULZE, W., DEUTSCHER, H.-J., UHLIG, V., and KUPPE, R., 1975, *J. Phys.*, **C1**, **36**, D1-379.
- [7] CLADIS, P. E., FINN, P. L., and GOODBY, J. W., 1984, *Liquid Crystals and Ordered Fluids*, Vol.4 edited by J. F. Johnson and R. S. Porter (New York: Plenum Press), p. 203.
- [8] GRIFFIN, A. C., FISHER, R. F., and HAVENS, S. J., 1978, *J. Am. chem. Soc.*, **100**, 6329.
- [9] DEUTSCHER, H.-J., KUSCHEL, F., BARGENDA, H., SCHUBERT, H., and DEMUS, D., 1973, DD-WP 106 120.
- [10] GRAY, G. W., and GOODBY, J. W., 1984, *Smectic Liquid Crystals* (Philadelphia: Heyden), p. 134.
- [11] GOODBY, J. W., BLENC, R., CLARK, N. A., LAGERWALL, S. T., OSIPOV, M. A., PIKIN, S. A., SAKURAI, T., YOSHINO, K., and ZEKS, B., 1991, *Ferroelectric Liquid Crystals, Preparation and Application* (Gordon and Breach), p. 99.
- [12] SAKURAI, Y., TAKENAKA, S., MIYAKE, H., MORITA, H., and TAKAGI, T., 1989, *J. chem. Soc. Perkin Trans. II*, 1199.
- [13] TAKENAKA, S., SAKURAI, Y., TAKEDA, H., IKEMOTO, T., MIYAKE, H., KUSABAYASHI, S., and TAKAGI, T., 1990, *Mol. Cryst. liq. Cryst.*, **178**, 103.
- [14] RATNA, B. R., KRISHNA PRASAD, S., SHASHIDHAR, R., HEPPKE, G., and PFEIFFER, S., 1985, *Mol. Cryst. liq. Cryst.*, **124**, 21.
- [15] SIGAUD, G., TINH, N. H., HARDOUIN, F., and GASPAROUX, H., 1981, *Mol. Cryst. liq. Cryst.*, **69**, 81.
- [16] HARDOUIN, F., ACHARD, M. F., TINH, N. H., and SIGAUD, G., 1985, *J. Phys. Lett.*, **46**, L-123.
- [17] TINH, N. H., and DESTRADE, C., 1981, *New. J. Chim.*, **5**, 337.
- [18] TINH, N. H., MALTHETE, J., and DESTRADE, C., 1981, *Mol. Cryst. liq. Cryst.*, **64**, 291.
- [19] TINH, N. H., 1985, *Mol. Cryst. liq. Cryst.*, **127**, 143.
- [20] OKAMOTO, H., PETROV, V. F., and TAKENAKA, S., 1999, *Liq. Cryst.*, **26**, 691.
- [21] MCMILLAN, W. L., 1973, *Phys. Rev. A*, **8**, 1921.
- [22] GRAY, G. W., 1977, in *Molecular Physics of Liquid Crystals*, edited by G. R. Luckhurst and G. W. Gray (New York: Academic Press), Chap. 1 and 13.
- [23] TAKEDA, H., SAKURAI, Y., TAKENAKA, S., MIYAKE, H., DOI, T., and KUSABAYASHI, S., 1990, *J. chem. Soc. Faraday Trans.*, **86**, 3429.
- [24] HAMMETT, L. P., 1970, *Physical Organic Chemistry* (London: McGraw-Hill), Chap. 11.
- [25] DUAN, M., OKAMOTO, H., PETROV, V. F., and TAKENAKA, S., 1999, *Liq. Cryst.*, **26**, 737.
- [26] OKAMOTO, H., TASAKA, T., DUAN, M., PETROV, V. F., and TAKENAKA, S. unpublished results.
- [27] CLADIS, P. E., 1998, *Liq. Cryst.*, **24**, 15 and references cited therein.
- [28] LYDON, J. E., and COAKLEY, C. J., 1975, *J. de Phys.*, **36**, C1-46.
- [29] HARA, M., IWAKABE, Y., TOCHIGI, K., SASABE, H., GARITO, A. F., and YAMADA, A., 1990, *Nature*, **344**, 228.
- [30] SMITH, D. P. E., HOBER, J. K. H., BINNING, G., and NEJOH, H., 1990, *Nature*, **344**, 641.
- [31] DUAN, M., OKAMOTO, H., PETROV, V. F., and TAKENAKA, S., 1998, *Bull. chem. Soc. Jpn.*, **71**, 2735.
- [32] SHASHIDHAR, R., RATNA, B. R., SURENDRANATH, V., RAJA, V. N., PRASAD, S. K., and NAGABHUSHAN, C., 1985, *J. Phys. Lett.*, **46**, L-445.
- [33] FONTES, E., HEINEY, P. A., HASELTINE, J. L., and SMITH, III A. B., 1986, *J. Phys.*, **47**, 1533.
- [34] TINH, N. H., HARDOUIN, F., and DESTRADE, C., 1982, *J. Phys.*, **43**, 1127.
- [35] MADHUSUDANA, N. V., SRIKANTA, B. S., and SUBRAMANYA, RAJ URS, M., 1983, *Mol. Cryst. liq. Cryst.*, **97**, 49.